International Journal of Computational Methods and Experimental Measurements
Vol. 12, No. 4, December, 2024, pp. 453-461
Journal homepage: http://iieta.org/journals/ijcmem

Effect of Friction Stir Processing on Microstructure and Mechanical Properties of In-Situ Composite A356/Al_3Ni Fabricated by Stir Casting

Noor Alhuda Baheer*, Muna Khethier Abbass, Israa Abd Al-Kadir Aziz

Department of Production Engineering and Metallurgy, University of Technology, Baghdad 10066, Iraq

Corresponding Author Email: pme.20.40@grad.uotechnology.edu.iq

Copyright: ©2024 The authors. This article is published by IIETA and is licensed under the CC BY 4.0 license (http://creativecommons.org/licenses/by/4.0/).

https://doi.org/10.18280/ijcmem.120414

Received: 19 October 2024
Revised: 28 November 2024
Accepted: 7 December 2024
Available online: 27 December 2024

Keywords:
Al-alloy A356, in-situ composite, Al_3Ni; fiction stir processing, stir casting, microstructure, tensile strength

ABSTRACT

A new technique for refining grains and creating surface composite materials was created using friction stir processing (FSP), which shows promise for improving the properties of metals. This technology can effectively overcome the limitations of methods that depend on melting. The work employed stir casting to produce in-situ composites, including an Al_3Ni reinforcing phase, Al alloy A356, and 15% weight percent pure Ni powder. The development of several phases of Al_3Ni, AlNi, and Al_3Ni_2, which are dispersed throughout the matrix of A356 alloy, was verified by XRD analytical examination. The objective was to determine how FSP impacted the stir-cast A356/Al3Ni in-situ composite's mechanical properties and microstructure. Porosity was successfully reduced, the α-Al dendrites were refined, the main Si phase and Al_3Ni were broken and fragmented, and the grain structure was improved by the FSP method. There was a consistent and equal distribution of in-situ Al_3Ni in the stir zone (SZ). There were no hazardous phases present when the particle and matrix came into contact. The application of FSP improved the tensile strength of the A356 alloy by 38.35% and the in-situ composite A356/Al_3Ni by 69.17%. It was found that the improvement in hardness was 14.47% for A356 alloy after FSP and 13.81% for in-situ composite A356/Al_3Ni compared to in-situ composite without FSP.

1. INTRODUCTION

High-strength aluminum alloys are the primary need for the automotive and aerospace sectors. Of the aluminum alloys' documented uses, the most promising ones are found in electronic packaging, aerospace constructions, parts for internal combustion engines and airplanes, power transmission towers, and a range of recreational goods. A356 is a cast alloy made of silicon, magnesium, and aluminum. Along with outstanding casting qualities, high corrosion resistance, and superb fluidity, this alloy is strong and ductile. In order to replace steel components, this alloy is widely used in the automotive, aerospace, and military industries. One of its main disadvantages in use is resistance [1].

In order to improve its quality, aluminum matrix composites, or AMCs, are designed to combine ceramic or hard particle reinforcement with aluminum (the matrix). The matrix has embedded reinforcing material. To enhance the mechanical and microstructure properties of AMCs, a wider range of production processes has been used throughout time. Since the fabrication method will define the final product's qualities, it is one of the most important variables in the production of AMCs. AMC manufacturing approaches may be divided into three main categories: in situ state fabrication, solid state fabrication, and ex-situ (liquid state fabrication) [2].

There are several methods for producing MMCs. For these, the dispersed phase can be introduced as an ex-situ phase or produced in situ. In-situ synthesis is the process of creating the dispersed phase inside the matrix, usually by means of an exothermic chemical reaction. Ex-situ, on the other hand, involves synthesizing the dispersed phase independently prior to its incorporation into the matrix [3].

Improved compatibility, stronger bonding between the reinforcements and the matrix, more thermodynamically stable reinforcements, and a defect-free reinforcement-matrix interface are only a few benefits of in-situ composites [4].

The primary problem in creating in-situ composites with conventional methods is the segregation of the reinforced particles produced in situ [5]. FSP combines the advantages of high temperature to aid the in-situ reaction, intense plastic deformation to promote mixing, and hot consolidation to produce a totally thick solid, making it an effective technique for producing in-situ composites [6, 7]. Because in situ-formed reinforced particles are nanoscale and significantly increase strength, the FSP approach is also appealing [8].

Furthermore, the in-situ produced particles at the interface can be successfully removed by the enormous plastic strain exerted in FSP. Due to their quick removal from the surface, the particles' ability to develop is constrained, resulting in nanoparticles [9]. Superplasticity, homogeneity of aluminum alloys and AMMCs, ex-situ and in-situ composites, metal foam production, and microstructural refinement of cast aluminum alloys are the main applications of FSP for microstructural modification in metallic materials [10, 11]. In

the stir-casting process, reinforcement is combined using a mechanical stirrer that creates a vortex in the matrix material. Stir casting's main advantages are its versatility, ease of usage, and capacity for large-scale manufacturing [12].

Balakrishnan et al. [13] investigated the characteristics and microstructure of AMCs in 2019. Al/(0-15 weight percent) Stir casting of pure metal powder into molten aluminum and FSP casting were used to create Al_3Fe AMCs. Particle reorganization into a homogeneous distribution following FSP. Defects like porosity in the casting were removed. Al3Fe particles had their sharp edges cut away and were softened into a nearly spherical form. The reinforced particles' severe plastic deformation and pinning action caused the grain size to decrease drastically. Following FSP, the dislocation density dramatically increased. Tensile strength and ductility increased as a result of the microstructural modifications.

Dinaharan et al. [14] examined the microstructure and characteristics of AMCs. Al/(0-15 weight percent) Al_2Cu AMCs were created by stir-casting molten aluminum with pure copper powder, then undergoing FSP. Microstructural alterations before and following FSP. Following FSP, the particle dispersion was reorganized into a homogenous distribution. Pores and other casting flaws were removed. The big particles of Al_2Cu were broken up into smaller ones. The grain size significantly decreased. Following FSP, the dislocation density significantly increased. Tensile strength and ductility improved as a result of the microstructural modifications. Fotoohi et al. [15] mechanically alloyed Ni, Ti, and C particles to create the reactive powder. The AA1050 alloy's channels were filled with reactive powders. The in-situ composite that was produced using six FSP runs demonstrated phase stability when exposed to high temperatures. Friction stir processed AA1050 without powder addition (30Hv, 90MPa) and Al-Al_3Ni/TiC hybrid composites outperformed AA1050 (25Hv, 84MPa) in terms of ultimate tensile strength of 179MPa, and hardness of 70Hv.

Gobalakrishnan et al. [16] used the stir-casting process. The ex-situ composite Al/SiC and in-situ composite Al/TiB_2 were produced. There were three different weight percentages of ceramic particles used: 4, 6, and 8%. The mechanical properties significantly improved when the concentration of reinforcing particles was raised from 4 to 8 weight percent. The in-situ composite TiB2 MMC has superior mechanical characteristics over the ex-situ composite SiC and the base metal, including tensile strength, hardness, and 0.2% proof strength. Kumar et al. [17] determined the impact of FSP on the kind of industrial waste particles in cast A356 alloy. Analysis showed that FSP decreased porosity, broke up α-Al dendrites, collapsed and re-distributed Si particles, and remodeled grains. In the SZ, the reinforced particles were uniformly dispersed and had little particle interaction. No destructive phase came into touch with the matrix or the particles. FSP produced microstructural alterations that enhanced the alloy's strength, ductility, and resistance to wear in comparison to the as-cast A356.

Daneshifar et al. [18] created in-situ composites of Al/Mg_2Si using FSP. In order to do this, a sample of pure magnesium was added to an Al-Si cast eutectic alloy via Friction Stir Processing (FSP). The Mg_2Si production process was investigated using a range of analytical methods. According to the findings, FSP is an appropriate method for creating Al/Mg_2Si composites. The resulting composite has a little increase in hardness, around 15% more than the original alloy that was subjected to FSP.

Using ultrasonic therapy with stir assistance, Sujith et al. [19] examined the Al_3Ti reinforcing phase's in-situ synthesis. In an Al-7075 alloy matrix, this technique improved the reinforcing particles' thermodynamic stability, uniformity, and wettability. Unlike the dendritic cells seen in the base alloy, the Al_3Ti particles stayed in their original location and acted as sites for the creation of more grains, resulting in the development of a non-dendritic globular form. Upon adding 2, 5, and 7 weight percent Al_3Ti, the α-Al dendrites' grain size decreased from 160µm to 65, 50, and 40µm, respectively.

Using the technique of stir casting, Chandrashekar et al. [20] created a composite material by combining B4C powders with aluminum alloy A 356. A356 alloy is combined with 2% B4C particles sized 44µm and 105µm in a 1:1 ratio, 4% B4C particles sized in a 3:1 ratio, and 6% B4C particles sized in a 1:3 ratio in three different composite compositions. There was a favorable link between the concentration of B4C particles and the hardness and tensile strength.

Kumar et al. [21] created surface composites using in situ AA5083-H111/Al-Fe. A two-pass friction stir process was applied to the AA5083 substrate, with the tool's movement direction being changed throughout the manufacturing process. After the second cycle, the tensile strength rose from 225.8MPa to 253.6MPa. Furthermore, during the first and second passes, the microhardness measurements revealed values of 123.3 and 128.3Hv, respectively.

Padmanaban et al. [22] investigated the friction stir welded process parameters on the tensile strength of dissimilar aluminum joints. They concluded that the tensile strength of the joint increases with the increase in tool rotational speed up to a limit of 1050rpm and decreases after that. The tensile strength of the joints is also increasing with the welding speed up to 15 mm/min; while further increase in speed caused a reduction of the tensile strength of the joints.

The goal of this research is to study the effect of friction stir processing on microstructure and mechanical properties of in-situ composite A356/Al_3Ni fabricated by stir casting. For that, an in-situ composite of A356/Al_3Ni has been created using stir casting to accomplish a reaction between molten aluminum and nickel powder. Furthermore, using FSP technology, the research seeks to improve the tensile properties, microhardness, and microstructure of the composite material.

2. MATERIALS AND METHODS

2.1 Materials used and specimen preparation

Aluminum alloy A356, which was made from commercially pure aluminum and an Al-11% Si master alloy, was the alloy utilized in the presented work. An electric resistance furnace was utilized to melt every material that was utilized. The furnace's temperature was predetermined at 750°C. After adjusting its chemical composition, the alloy was heated and then poured into the metallic mold. Utilizing a Thermo ARL 3460-type optical emission spectrometer, the chemical makeup of the generated A356 aluminum alloy was investigated. The Al alloy A356's chemical composition is listed in Table 1. Using aluminum alloy A356 as the matrix and 1.0175-µm-sized micro-Ni particles as reinforcement, Al_3Ni in-situ composites with Ni 15wt% have been created.

Al alloy A356 was placed in an alumina crucible in an electric furnace at 750°C, which is higher than the liquidus temperature. After holding the melt at this temperature for

around 15 minutes to homogenize, a flux of 1% CaF_2 was added to the melt to remove the impurities (as slag) from the melt. Ni particulates have been added, warped in an Al foil, and pre-heated to 350°C for 1hr for the purpose of removing moisture and added gradually to the molten alloy along with an electric stirrer at 500rpm to achieve good dispersion of reinforcing within melt and degassing using an inert gas (argon), as illustrated in Figure 1, After that the melt is poured into the cavity of the pre-heated metallic rectangular mold at 250°C, which has dimensions of 10×100×150mm.

Table 1. Chemical composition of prepared A356 alloy

Element (wt%)	Actual Value Measured	Standard Value
Si	7.38	6.6-7.5
Fe	0.5	0.6
Cu	0.2	0.25
Mn	0.1	0.35
Mg	0.4	0.20-0.45
Zn	0.3	0.35
Ti	0.02	0.25
Al	balance	balance

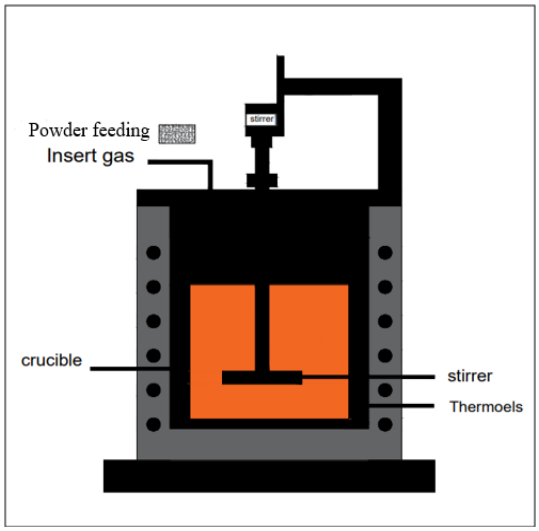

Figure 1. Stir stir-casting technique used in this work

The FSP was carried out on a CNC vertical machining center that was computer numerically controlled model Knuth Werkzeugmaschinen GmbH, Germany. Following a series of tests, the FSP's fixed rotation speed of 1250rpm, travel speed of 75mm/min, and plunge depth of 3.1mm were adopted. All experiments were performed at room temperature. Each FSP experiment utilized a single pass. High-speed steel (HSS) was used to develop and build the FSP tool. A 6 mm diameter pin that is 3mm deep and a 16mm shoulder make up the geometric shape.

The specimens obtained from the castings and friction stir-treated plates were examined using an optical microscope for microstructural characterization. The wet grinding process included the use of water and SiC emery paper with different grit sizes, including 320, 500, 600, 800, 1000, and 1200. Lubricant, a special polishing cloth, and 0.5µm diamond paste were used to polish the specimen. Using Keller's reagent, a solution consisting of 95ml H_2O, 2.5ml HNO_3, 1.5ml HCl, and 1.0ml HF, the specimens were etched. Following a cleaning procedure, the objects were exposed to a moisture removal process.

A scanning electron microscope (SEM) device, namely the VEGA3LMe model, with a high-resolution mode and Oxford MAX3 model-based energy dispersive spectroscopy (EDS), was employed in this study. To identify the various phases contained in the microstructures, the specimens' X-ray diffraction (XRD) patterns were generated using a diffractometer (Bruker D8) using Cu-K radiation.

The digital micro-hardness tester Laryee HVS-1000 was used to conduct the Vickers hardness test. An applied force of 200 grams was used for 15 seconds. The tensile specimens were manufactured in accordance with ASTM standard E8/E8M-09 and evaluated at room temperature using a computer-controlled universal testing apparatus (INSTRON, 8810). The speed throughout testing was 1.0mm per minute. The broken tensile specimens' shattered surfaces were examined using a scanning electron microscope.

3. RESULTS AND DISCUSSION

3.1 Microstructure

A micrograph of the A356 Al alloy sections as cast following FSP is shown in Figure 2 (a). Four different zones are clearly seen in the FSP specimen. The SZ, a thermomechanically treated area, is distinguished by its small grain size and equiaxed or homogenized grain structure. There are three zones present: the thermomechanically affected zone (TMAZ), the heat-affected zone (HAZ), and the friction stir-treated zone. The expanded grain in the TMAZ is due to thermomechanical deformation. The HAZ's grain structure is analogous to that of the base metal (BM).

The area that the FSP process does not affect is the base metal (BM). The A356 Al alloy features a main α-Al phase in the form of a dendritic structure, which appears as white areas. It also has an Al-Si eutectic, which appears as black regions. In Figure 2 (b), the eutectic phase is seen as a continuous phase encircling the α-Al dendrites, whereas the Si particles are fractured into irregular fragments inside the base metal. Following the process of FSP, the microstructure undergoes a full transformation, resulting in a changed structure that is desired. As seen in Figure 2 (c), the cast matrix alloy's dendritic microstructure experienced considerable severe plastic deformation before being refined. Silicon was altered, and grains were refined using Friction Stir Processing (FSP). Subtle microstructure alterations were seen in the SZ, which had a globular shape with small Si particles. In the stir zone, these particles were notably more uniformly dispersed. At high temperatures, Friction Stir Processing (FSP) causes considerable plastic deformation of the material in the stir zone. When the material was stressed at high temperatures, dynamic recrystallization took place, creating nucleation sites [23].

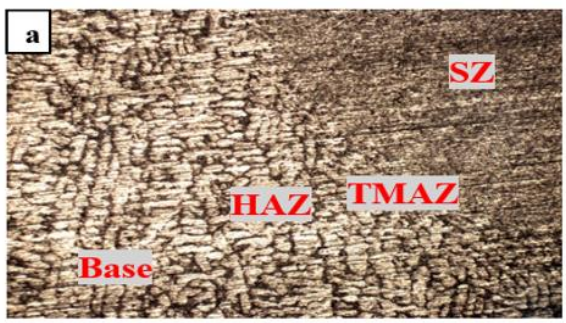

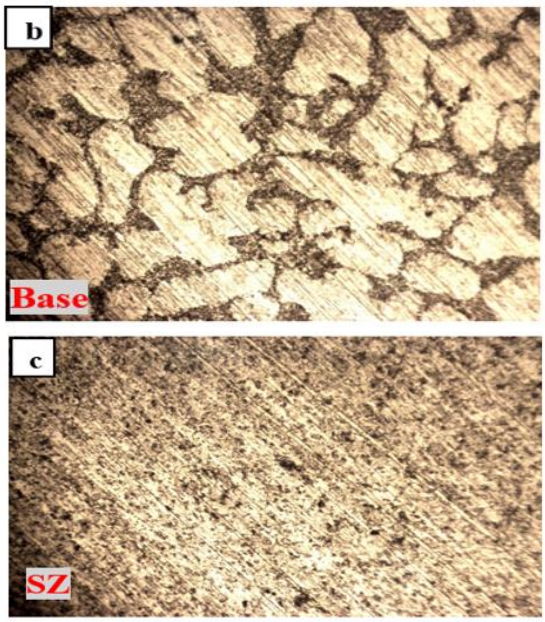

Figure 2. Optical micrographs showing the microstructure of the base A356 after FSP, showing (a) base metal, HAZ, TMAZ, and SZ at 100 x, (b) Base metal at 400 x, and (c) SZ at 400 x

Following FSP, optical micrographs of the in-situ composites A356/Al_3Ni are displayed in Figure 3 (a). The small Al_3Ni particles in the matrix alloy are distributed uniformly. Figure 3 (b) shows that following FSP, the Al_3Ni was generated in situ and evenly dispersed throughout the Al matrix. Along with Al_3Ni, intermetallic compounds of various sizes and shapes were also seen in the composites [19, 24].

Figures 4 (a) and 4 (b) show SEM micrographs of the microstructures of the basic alloy A356 and in situ composites containing (15%) Ni. The primary α-Al phase and Al-Si eutectic make up the alloy A356 initial microstructure, as can be seen from Figure 4 (b) Al_3Ni intermetallic compound various shapes of agglomeration of Al_3Ni intermetallic compound have been observed in the 15wt% Ni. These findings are consistent with those of Abbass et al. [25-27].

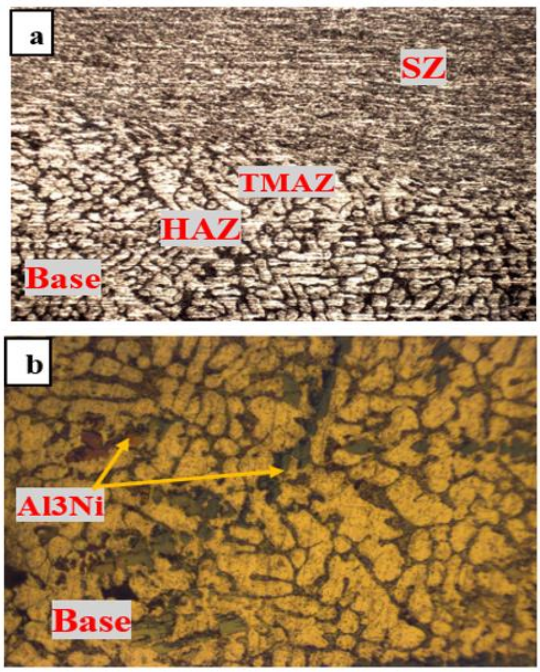

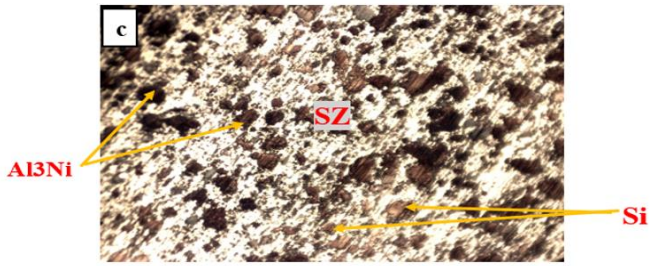

Figure 3. Optical micrographs showing the microstructure of In- situ composite A356/Al_3Ni after FSP (a) base, HAZ, TMAZ, and SZ at 100 x (b) Base metal at 400 x (c) SZ at 400 x

Figure 4 (c) shows scanning electron microscopy (SEM) pictures of the microstructure of A356 cast after friction stir processing. This process resulted in the refinement of aluminum dendrites, the repositioning of small and equiaxed silicon particles within the aluminum matrix, and the visible disintegration of fibrous silicon particles [28].

Figure 4 (d) depicts the microstructure of the friction-stir-processed zone of A356/Al_3Ni AMC. Uniformizes Ni particle distribution in A356/Al_3Ni in situ composites. Friction stir processing (FSP) has been shown to achieve complete homogeneity. The rotating instrument produces enough heat and circumferential force to uniformly distribute the nickel (Ni) particles throughout the larger region. Regarding the parameters of metal flow during friction stir processing of A356/Al_3Ni in situ composites in SZ. A single FSP round was enough to improve the distribution and break up particle segregation at grain boundaries [29].

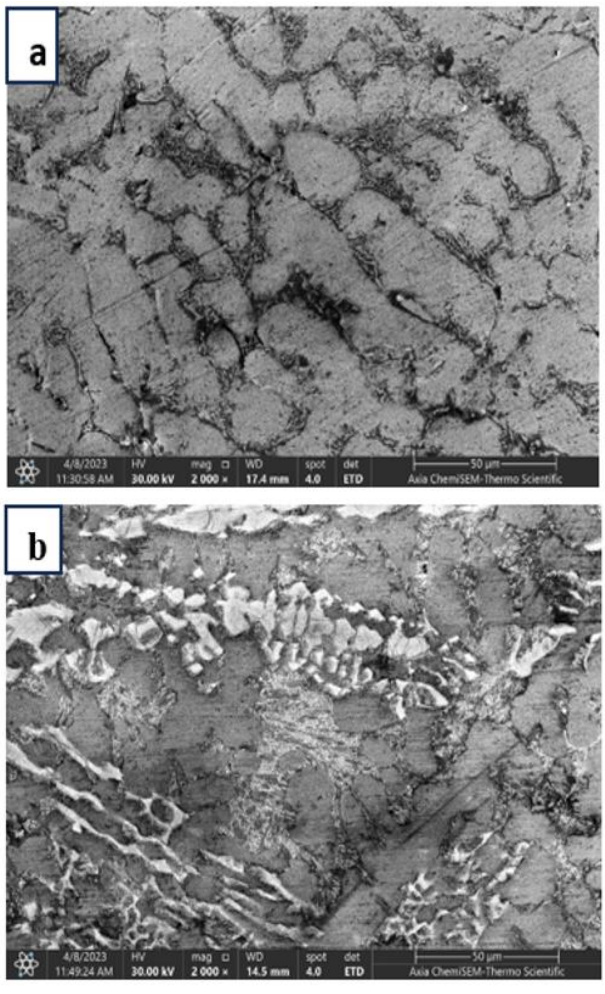

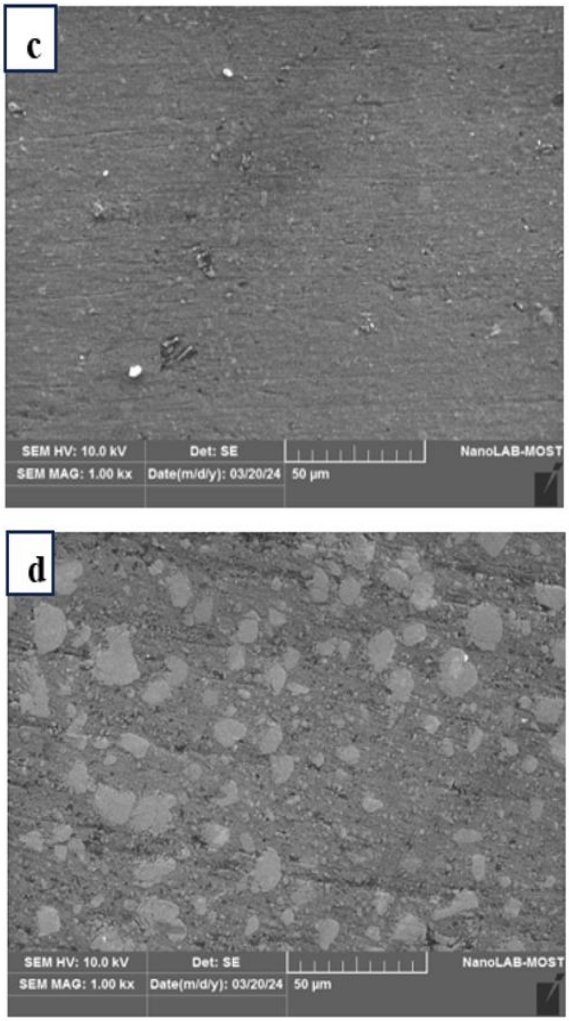

Figure 4. SEM micrographs of A 356 as cast before and after FSP. (a) A356 as cast, (b) A356/Al_3Ni as cast, (c) A356 after friction stir processed, and (d) A356/Al_3Ni after friction stir processed

3.2 X-ray diffraction analyses

Figures 5 and 6 show the XRD patterns of cast base Al alloy A356 specimens and in situ composite specimens (15wt% Ni). In the XRD pattern of cast Al alloy A356, it was discovered that the presence of Al phases is evident and greatest, while the intensity of Si peaks is lesser. Additionally, the emergence of peaks of the intermetallic compound Al3Ni, Al Ni, and Al_3Ni_2 phase is exhibited in the XRD pattern of in-situ composite of A356- 15wt% Ni, as observed by Manjunatha et al. [30].

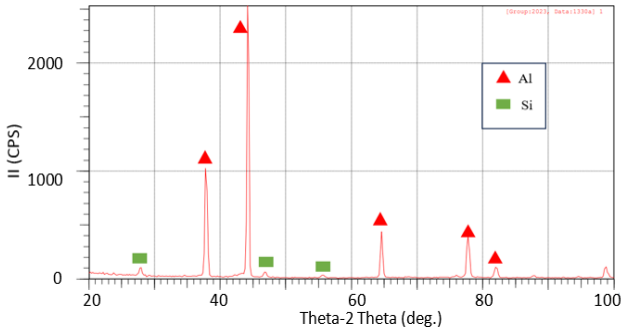

Figure 5. XRD pattern of cast A356 Al alloy

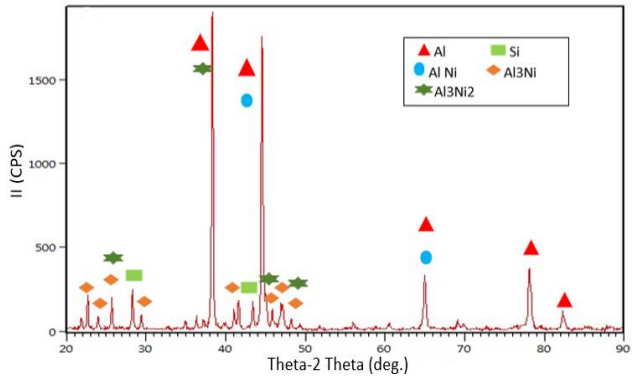

Figure 6. XRD pattern of in-situ composite (A356-15%Ni)

3.3 Microhardness

The treated zone's cross-section was measured using the axis of the hardness profile. It seems that FSP might change the distribution of hardness on any particular specimen in light of the earlier microstructural discoveries. FSPed specimens' microstructure is made up of four main areas: The BM, HAZ, SZ, and TMAZ. Figure 7 shows the hardness profile of the specimens (A356 and A356/Al_3Ni) before and after the friction stir operation. We measured the microhardness of the matrix of the in-situ composites that were cast and friction stir processed (FSPed). Each hardness measurement is calculated as the average of at least three readings. The hardness increases considerably after FSP as a result of the refining grain and dynamically recrystallized zone. The A356/Al_3Ni has a hardness of 152 and 173 HV, whereas the as-cast A356 has a hardness of 76 and 87 HV before and after the first FSP pass, respectively. Dispersion hardening is more successful after FSP because of the improved uniformity of particle distribution. The hardness is also improved by the high dislocation density and particle refinement [31, 32].

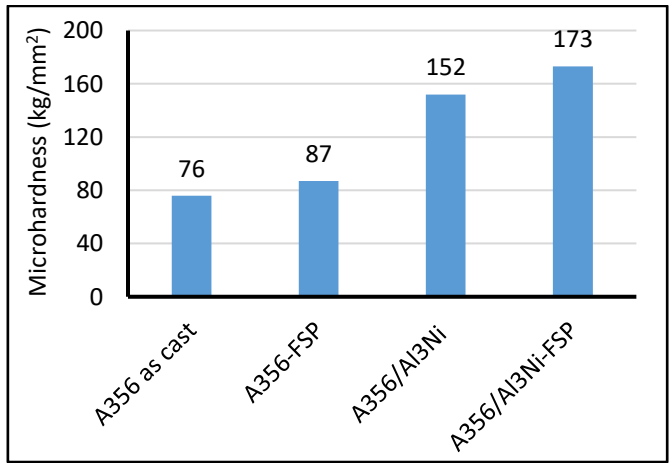

Figure 7. Hardness values of as-cast A356 alloy and in-situ composites

3.4 Tensile properties

Table 2 summarizes the tensile characteristics of the as-cast and FSPed in situ composites, and Figure 8 depicts the connection between stress and strain. After doing FSP, stamina shows a discernible improvement. The tensile strength is also significantly enhanced following FSP, as illustrated in Figure 9. The strength of the A356 as cast and in-situ

composite A356/Al_3Ni after FSP is high compared to A356 as cast before FSP, as evidenced by Table 2. Numerous strengthening mechanisms occurred in base A356 and in situ composite A356/Al_3Ni after FSP, including precipitation hardening that is dispersed throughout the Al-matrix. This is due to the following variables, in addition to the dispersion strength produced by the distribution of Al_3Ni, AlNi, and Al_3Ni_2, which hinder the movement of dislocations and boost the mechanical characteristics.

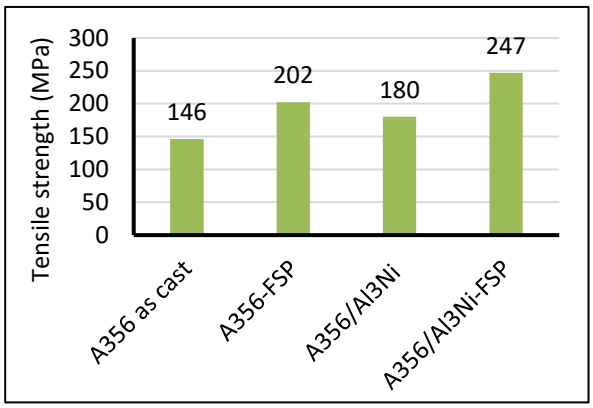

Figure 8. Tensile strength as-cast of A356 alloy and composites

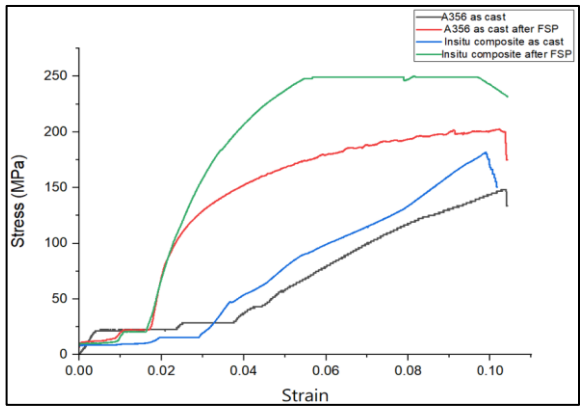

Figure 9. Stress-strain curve for A356 as cast and in-situ composite A356/Al_3Ni before and after FSP

Table 2. Tensile test results for the specimen of base alloy A356 and in-situ composites before and after FSP

Specimen	Tensile Strength (MPa)	Yield Strength (MPa)	Elongation (%)	Improvement%
A356 as cast	146	70	10.32%	-
A356+FSP	202	130	17.78%	38.35%
A356/Al_3Ni	180	90	9.98%	23.28%
A356/Al_3Ni+FSP	247	150	9.24%	69.17%

Additionally, the mechanics of grain boundaries were strengthened in the agitation zone and base metal, resulting in improved dispersion strengthening. As per the Hall–Petch relationship, the strength is further enhanced as a result of the finer particle size that is obtained after FSP. These results agree with the studies [33, 34], which carried out FSP on wrought and cast aluminum alloy. The properties are also enhanced by the FSP removal of casting defects [35, 36].

3.5 Fracture analysis

The fracture surface was examined using a scanning electron microscope (SEM), as shown in Figure 10. The A356 and A356/Al_3Ni tensile specimens' fracture surfaces are depicted in the SEM micrograph both in their cast and post-friction stir processing (FSP) states.

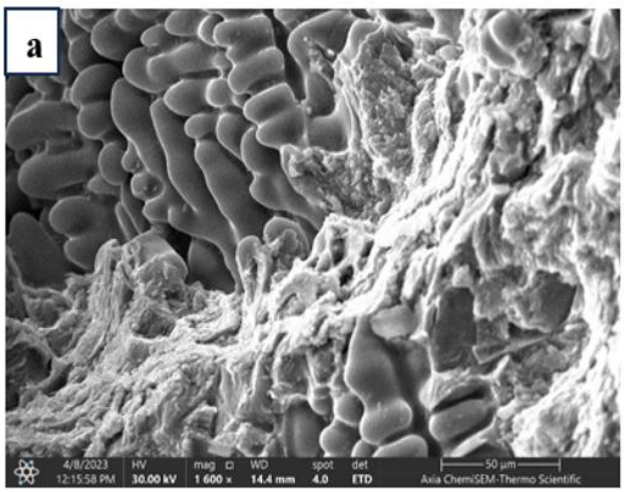

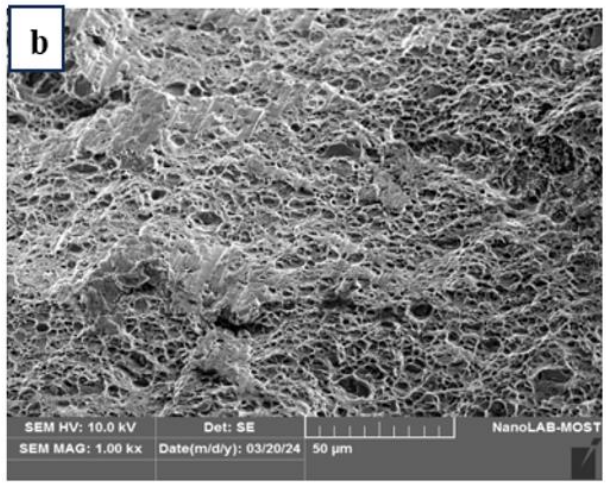

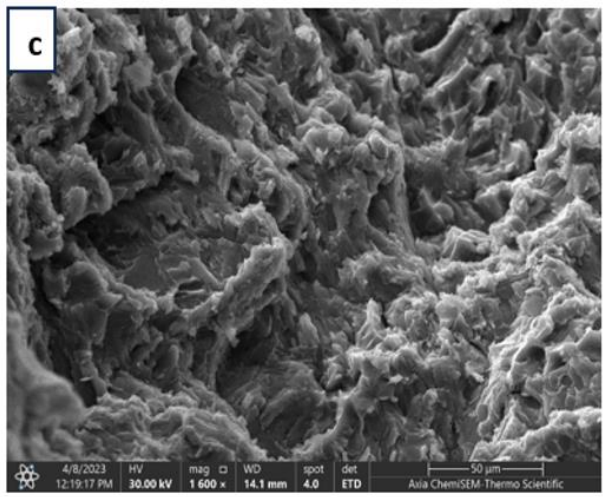

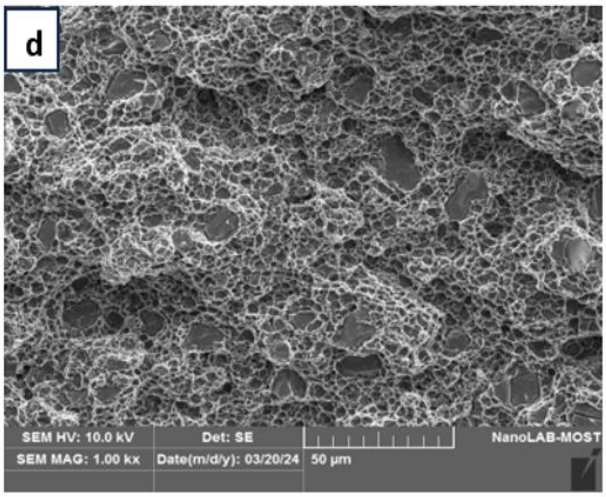

Figure 10. Fracture surface (a) A356 as cast, (b) A356 as cast after FSP, (c) A 356/Al_3Ni in situ composite as cast, (d) A 356/Al_3Ni in-situ composite after FSP

The in-situ composites (Figures 10 (a) and (c)) do not exhibit distinct dimple development. The crack's upper surface is rather level and flat. Holes have been noticed on the split surface. Based on these numbers, it looks like the group failed weakly. There is not much solid evidence that the metal matrix changed shape significantly before it collapsed. The crack surfaces of alloys that have been processed with friction stir (Figure 10 (b) and (d)), on the other hand, show that the aluminum matrix has been deformed plastically. There is a clear pattern of small depressions on the broken surface. It looks like the breaking mode is flexible [37, 38].

4. CONCLUSION

The work employed stir casting to produce in-situ composites including an Al_3Ni reinforcing phase, Al alloy A356, and 15% weight percent pure Ni powder and determine how FSP impacted the stir-cast A356/Al_3Ni in-situ composite's mechanical properties and microstructure. From the present investigation, the following important conclusions are derived:

- Modification and refinement microstructure was noticed in base alloy A356 and in-situ composite after FSP at the best conditions.
- Because of friction heat and plastic deformation of the FSPed region, FSP enhanced the mechanical properties of A356 base alloy and in-situ composite A356/Al3Ni. It made A356 and in-situ composite A356/Al3Ni harder by 14.47% and 13.81%, respectively, and increased their tensile strength by 38.35% and 69.17%, respectively.
- Many strengthening mechanisms occurred of base alloy and in-situ composite such as dispersion hardening by forming intermetallic phase of Al3Ni particulate, grain boundaries hardening by dynamic recovery and recrystallization in the stir zone, severe plastic deformation in stir zone and TMAZ, which improve largely the mechanical properties.
- From SEM examination of the fracture surface of tensile test specimens, it was observed that the ductile fracture with dimples before FSP while brittle fracture with cleavage mode in specimens after FSP.

REFERENCES

[1] Roy, P., Singh, S., Pal, K. (2019). Enhancement of mechanical and tribological properties of SiC-and CB-reinforced aluminium 7075 hybrid composites through friction stir processing. Advanced Composite Materials, 28(sup1): 1-18. http://doi.org/10.1080/09243046.2017.1405596

[2] Ervina Efzan, M.N., Siti Syazwani, N., Al Bakri, A.M. (2016). Fabrication method of aluminum matrix composite (AMCs): A review. Key Engineering Materials, 700: 102-110. https://doi.org/10.4028/www.scientific.net/KEM.700.102

[3] Mussatto, A., Ahad, I.U., Mousavian, R.T., Delaure, Y., Brabazon, D. (2021). Advanced production routes for metal matrix composites. Engineering Reports, 3(5): e12330. http://doi.org/10.1002/eng2.12330

[4] Tjong, S.C., Ma, Z.Y. (2000). Microstructural and mechanical characteristics of in situ metal matrix composites. Materials Science and Engineering: R: Reports, 29(3-4): 49-113. https://doi.org/10.1016/S0927-796X(00)00024-3

[5] Bauri, R. (2014). Optimization of process parameters for friction stir processing (FSP) of Al-TiC in situ composite. Bulletin of Materials Science, 37: 571-578. http://doi.org/10.1007/s12034-014-0692-z

[6] Hsu, C.J., Chang, C.Y., Kao, P.W., Ho, N.J., Chang, C. P. (2006). Al-Al3Ti nanocomposites produced in situ by friction stir processing. Acta Materialia, 54(19): 5241-5249. https://doi.org/10.1016/J.ACTAMAT.2006.06.054

[7] Kumar, P.A., Madhu, H.C., Pariyar, A., Perugu, C.S., Kailas, S.V., Garg, U., and Rohatgi, P. (2020). Friction stir processing of squeeze cast A356 with surface compacted graphene nanoplatelets (GNPs) for the synthesis of metal matrix composites. Materials Science and Engineering: A, 769: 138517. https://doi.org/10.1016/j.msea.2019.138517

[8] Tjong, S.C. (2007). Novel nanoparticle-reinforced metal matrix composites with enhanced mechanical properties. Advanced Engineering Materials, 9(8): 639-652. https://doi.org/10.1002/adem.200700106

[9] Sharma, V., Prakash, U., Kumar, B.M. (2015). Surface composites by friction stir processing: A review. Journal of Materials Processing Technology, 224: 117-134. https://doi.org/10.1016/j.jmatprotec.2015.04.019

[10] Sahu, M.K., Sahu, R.K. (2018). Fabrication of aluminum matrix composites by stir casting technique and stirring process parameters optimization. Advanced Casting Technologies. Intechopen, 111-122. http://doi.org/10.5772/intechopen.73485

[11] Alishavandi, M., Ebadi, M., Alishavandi, S., Kokabi, A.H. (2020). Microstructural and mechanical characteristics of AA1050/mischmetal oxide in-situ hybrid surface nanocomposite by multi-pass friction stir processing. Surface and Coatings Technology, 388: 125488. https://doi.org/10.1016/j.surfcoat.2020.125488

[12] Gangil, N., Siddiquee, A.N., and Maheshwari, S. (2017). Aluminum based in-situ composite fabrication through friction stir processing: A review. Journal of Alloys and Compounds, 715: 91-104. https://doi.org/10.1016/j.jallcom.2017.04.309

[13] Balakrishnan, M., Dinaharan, I., Palanivel, R.,

Sathiskumar, R. (2019). Effect of friction stir processing on microstructure and tensile behavior of AA6061/Al3Fe cast aluminum matrix composites. Journal of Alloys and Compounds, 785: 531-541. https://doi.org/10.1016/j.jallcom.2019.01.211
[14] Dinaharan, I., Balakrishnan, M., Selvam, J.D.R., Akinlabi, E.T. (2019). Microstructural characterization and tensile behavior of friction stir processed AA6061/Al2Cu cast aluminum matrix composites. Journal of Alloys and Compounds, 781: 270-279. https://doi.org/10.1016/j.jallcom.2018.12.091
[15] Fotoohi, H., Lotfi, B., Sadeghian, Z., Byeon, J.W. (2019). Microstructural characterization and properties of in situ Al-Al3Ni/TiC hybrid composite fabricated by friction stir processing using reactive powder. Materials Characterization, 149: 124-132. https://doi.org/10.1016/j.matchar.2019.01.024
[16] Gobalakrishnan, B., Rajaravi, C., Udhayakumar, G., Lakshminarayanan, P.R. (2021). Effect of ceramic particulate addition on aluminium based ex-situ and in-situ formed metal matrix composites. Metals and Materials International, 27: 3695-3708. http://doi.org/10.1007/s12540-020-00868-6
[17] Kumar, H., Prasad, R., Kumar, P., Tewari, S.P., Singh, J.K. (2020). Mechanical and tribological characterization of industrial wastes reinforced aluminum alloy composites fabricated via friction stir processing. Journal of Alloys and Compounds, 831: 154832. https://doi.org/10.1016/j.jallcom.2020.154832
[18] Daneshifar, M.H., Papi, A., Alishahi, M. (2021). Fabrication of Al-Si/Mg2Si in-situ composite by friction stir processing. Materials Letters, 282: 128832. https://doi.org/10.1016/j.matlet.2020.128832
[19] Sujith, S.V., Kim, H., Mulik, R.S., Park, H., Lee, J. (2022). Synergistic effect of in-situ Al-7075/Al3Ti metal matrix composites prepared via stir-assisted ultrasonic melt processing under dynamic nucleation. Metals and Materials International, 28(9): 2288-2303. http://doi.org/10.1007/s12540-021-01143-y
[20] Chandrashekar, J.R., Annaiah, M.H., Chandrashekar, R. (2021). Microstructure and mechanical properties of aluminum cast alloy A356 reinforced with dual-size B4C particles. Frattura ed Integrità Strutturale, 15(57): 127-137. http://doi.org/10.3221/IGF-ESIS.57.11
[21] Singhal, V., Jain, V.K., Raman, R.S., Patharia, D., Mittal, V., Mishra, S., Kumar, H. (2024). Optimization of friction stir processing parameters for improving structural and mechanical properties in in situ AA5083-H111/Al-Fe composites. Proceedings of the Institution of Mechanical Engineers, Part C: Journal of Mechanical Engineering Science, 238(10): 4477-4490. http://doi.org/10.1177/09544062231211672
[22] Padmanaban, R. Balusamy, V., Nouranga, K.N. (2015). Effect of process parameters on the tensile strength of friction stir welded dissimilar aluminum joints. Journal of Engineering Science and Technology, 10(6): 790-801.
[23] Dhanasekaran, R., Kumar, K.S. (2015). Microstructure, mechanical properties of A356/Li aluminum alloy fabrication by stir casting method. International Journal of Applied Engineering Research, 10(50): 416-419.
[24] Ma, Z.Y., Sharma, S.R., Mishra, R.S. (2006). Effect of friction stir processing on the microstructure of cast A356 aluminum. Materials Science and Engineering: A, 433(1-2): 269-278. https://doi.org/10.1016/j.msea.2006.06.099
[25] Abbass, M.K. (2010). Effect of Cd on microstructure and dry sliding wear behavior of (Al-12% Si) alloy. The Journal of Engineering Research, 7(1): 1-10. https://doi.org/10.24200/tjer.vol7iss1pp1-10
[26] Abbass, M.K. (2018). Laser surface treatment and modification of aluminum alloy matrix composites. Lasers in Manufacturing and Materials Processing, 5(2): 81-94. https://link.springer.com/article/10.1007/s40516-018-0054-6
[27] Abbass, M.K., Muhammed, O.S. (2012). Study on the effect of casting pressure on the wear resistance of Al-Si alloy prepared by squeeze casting. Journal of King Abdulaziz University, 23(1): 3. http://doi.org/10.4197/Eng.23-1.1
[28] Zhao, Y., Kai, X., Chen, G., Lin, W., Wang, C. (2016). Effects of friction stir processing on the microstructure and superplasticity of in-situ nano-ZrB2/2024Al composite. Progress in Natural Science: Materials International, 26(1): 69-77. http://doi.org/10.1016/j.pnsc.2016.01.009
[29] Abbass, M.K., Sharhan, N.B. (2023). Characteristics of Al6061-SiC-Al2O3 surface hybrid composites fabricated by friction stir processing. Journal of Materials and Engineering, 1(4): 147-158. https://doi.org/10.61552/jme.2023.04.002
[30] Manjunatha, H.S., Mallesh, G., Pradeepkumar, V.G. (2020). Mechanical characterization of aluminum-TiB2 metal matrix composites by in-situ method. International Research Journal of Engineering and Technology, 7: 298-304.
[31] Abbass, M.K., Baheer, N.A. (2020). Effect of SiC particles on microstructure and wear behavior of AA6061-T6 aluminum alloy surface composite fabricated by friction stir processing. IOP Conference Series: Materials Science and Engineering, 671(1): 012159. http://doi.org/10.1088/1757-899X/671/1/012159
[32] Mohammed, M.H., Subhi, A.D. (2021). Exploring the influence of process parameters on the properties of SiC/A380 Al alloy surface composite fabricated by friction stir processing. Engineering Science and Technology, an International Journal, 24(5): 1272-1280. https://doi.org/10.1016/j.jestch.2021.02.013
[33] Abbass, M.K., Sharhan, N.A.B. (2019). Optimization of friction stir processing parameters for Aluminum alloy (AA6061-T6) using Taguchi method. Al-Qadisiyah Journal for Engineering Sciences, 12(1). https://doi.org/10.30772/qjes.v12i1.580
[34] Abdel-Aziz, A.I., AbouTaleb, A.S., Farahat, A.I., El-Baradie, Z.M. (2018). Effect of friction stir processing parameters on mechanical properties and microstructural evolution for Al-11.4Si-4Cu-0.5Fe. World of Metallurgy, 71(5): 263-272.
[35] Jlood, K.K., Abbass, M.K., Hanoon, M.M. (2024). Effect of friction stir processing parameters on microstructure and mechanical properties of aluminum alloy AA6061-T6: Experimental and statistical study. Salud, Ciencia y Tecnología-Serie de Conferencias, 3: 862. http://doi.org/10.56294/sctconf2024862
[36] Baheer, N.A., Abbass, M.K., Aziz, I.A.A.A.K. (2024). Microstructure and wear behavior of in-situ composite A356/Al3Ni fabricated by stir casting. In AIP Conference Proceedings. AIP Publishing, 3229(1).

https://doi.org/10.1063/5.0236495
[37] Mahmoud, T.S., Mohamed, S.S. (2012). Improvement of microstructural, mechanical and tribological characteristics of A413 cast Al alloys using friction stir processing. Materials Science and Engineering: A, 558: 502-509. https://doi.org/10.1016/j.msea.2012.08.036
[38] Saini, N., Dwivedi, D.K., Jain, P.K., Singh, H. (2015). Surface modification of cast Al-17% Si alloys using friction stir processing. Procedia Engineering, 100: 1522-1531. https://doi.org/10.1016/j.proeng.2015.01.524

NOMENCLATURE

FSP	Friction stir processing
FSW	Friction stir welding
XRD	X-ray diffraction
SEM	Scanning electron microscope
SZ	Stir zone
TMAZ	Thermo-mechanically affected zone
HAZ	Heat affected zone
BM	Base metal
MMC	Metal matrix-composites
AMCs	Aluminum matrix composites
HSS	High-speed steel